

● *Original Contribution*

## IN VIVO BREAST TUMOR DETECTION USING TRANSIENT ELASTOGRAPHY

J. BERCOFF,\* S. CHAFFAI,\* M. TANTER,\* L. SANDRIN,\* S. CATHELIN,\* M. FINK,\*  
J. L. GENNISSON\* and M. MEUNIER<sup>†</sup>

\*Laboratoire Ondes et Acoustique, E.S.P.C.I., Université Paris VII, U.M.R. 7587 C.N.R.S 1503, Paris, France; and

<sup>†</sup>Institut Curie, Service de Radio diagnostique, Paris, France

(Received 18 October 2002; revised 22 April 2003; in final form 29 April 2003)

**Abstract**—This paper presents first *in vivo* experiments for breast tumor detection using transient elastography. This technique has been developed for detection and quantitative mapping of hard lesions in soft tissues. It consists in following the propagation inside soft tissues of very low-frequency shear waves ( $\sim 60$  Hz) generated by a vibrating system located at the body surface. Because transient shear waves propagate through the medium in less than 0.1 s, the shear propagation imaging is performed with an ultrafast echographic scanner able to reach frame rates up to 6000 Hz. The local shear wave speed is directly linked to the local shear Young's modulus of the medium. The shear elasticity map of the medium can then be computed using an inversion algorithm. *In vivo* experiments were conducted on 15 women who had palpable breast lesions. For clinical adaptability reasons, shear waves were generated by the surface of the ultrasound (US) imaging transducer itself, which was linked to a mechanical vibrator. Our preliminary *in vivo* results demonstrate the clinical applicability of the transient elastography technique for breast lesion detection. (E-mail: michael.tanter@espci.fr) © 2003 World Federation for Ultrasound in Medicine & Biology.

**Key Words:** Ultrasound, Transient elastography, Breast cancer, Shear waves, Young's modulus.

### INTRODUCTION

Body palpation is a well-known medical method used by physicians to assess organs stiffness. External forces applied on the body surface induce tissue displacements from which elastic constants can be subjectively estimated. In the last decade, several ultrasound (US) (Ophir et al. 2000; Parker and Lerner 1992; Levinson et al. 1995; Yamakoshi et al. 1990; Catheline et al. 1999; Sandrin et al. 2002a, 2002b; Tanter et al. 2002) or magnetic resonance imaging (MRI)-based techniques (Muthupillari et al. 1995; Sinkus et al. 2000) were proposed to estimate the mechanical response of in depth tissues to external excitations. In US, these techniques can be classified according to the kind of mechanical excitation used: static compression (Ophir et al. 1991, 1996, 2000), dynamic vibrations (Parker and Lerner 1992; Levinson et al. 1995) or pulsed excitations (Catheline et al. 1999; Sandrin et al. 1999, 2002a, 2002b;

Tanter et al. 2002). The work presented in this paper refers to a pulsed excitation-based technique called transient elastography. The low-frequency ( $\sim 60$  Hz) pulsed excitation induces a shear wave in the tissues whose local velocity (typically from 1 to 10 m/s) is directly related to the local Young's modulus. Displacements induced in the medium by the shear wave are measured with a single ultrasonic array connected to an ultrafast imaging system (up 6000 images/s), able to follow the shear wave propagation. The ultrafast frame rate is achieved by reducing the emitting mode to a single plane wave insonification and storing all backscattered radio-frequency (RF) data in memories. This plane wave insonification for ultrafast frame rate was first introduced by Shattuck (1984) and recently investigated for elastography by Sandrin et al (1999, 2002a, 2002b). Signal processing for shear elasticity estimation is performed in a postacquisition process. Compared with static elastography or sonoelastography, this technique has the advantage of being insensitive to patient motion and boundary condition artefacts because of its real-time capabilities (acquisition time of a few 10s of ms). Furthermore, it does not require to take into account compressional

Address correspondence to: Dr. Mickael Tanter, Laboratoire Ondes et Acoustique, E.S.P.C.I., Université Paris VII, U.M.R. 7587 C.N.R.S 1503, 10 rue Vauquelin 75231 Paris cedex 05 France. E-mail: michael.tanter@espci.fr

waves and mode conversions, as happens in sonoelastography. In previous works (Sandrin et al. 1999, 2002a, 2002b), transient elastography has been tested and validated as a quantitative technique to provide soft tissue elasticity maps. The work presented in this paper intends to test the adaptability of the technique to clinical conditions for breast tumor detection. Experiments were conducted on women who had palpable breast lesions. In most of the cases, the lesions had a different echogenicity than surrounding tissues and could be visualized with standard us imaging, giving us a spatial reference to validate our results. In the first section, a brief description of the experimental setup and the signal processing used for the clinical implementation is given. *In vivo* results are presented in the second section. Finally, results and clinical capabilities of the technique are discussed in the last section.

## MATERIALS AND METHODS

### Electronics

Though low-frequency shear waves propagate at a low speed of a few  $\text{ms}^{-1}$  in soft tissues, the frame rate of the detection system must be higher than 1000 frames/s to be able to follow their propagation on a mm scale. Standard US scanners are limited to about 50 frames/s which is not sufficient to detect shear wave propagation. To overcome this problem, an ultrafast electronic system based on a time-reversal mirror electronic technology was developed in our laboratory (Sandrin et al. 1999, 2002a, 2002b). This ultrafast scanner is a fully programmable multichannel system made of 128 channels connected to the ultrasonic array. Each element possesses its own emission/reception electronic board and 2 Mb of memory to store emission and reception signals. The ultrafast frame rate is achieved by reducing the emitting mode to a single plane-wave insonification. This technique allows acquiring echographic images at a pulse repetition that can reach 6000 Hz. All backscattered RF echoes are stored in the 2-Mb memory of each channel and then transferred to a computer after acquisition. The signals are sampled at 50 MHz and digitized with 9-bit resolution after an analogic logarithm amplification. The beam-forming and signal processing of the RF data are done on the computer during a postacquisition process. A typical number of 200–300 data sets (for a 6-cm depth) can be acquired during one acquisition sequence. The ultrafast scanner is connected to a Vermon 4.3-MHz US array (0.33-mm pitch, 10-mm elevation, geometrically focused in elevation at 60 mm).

Avoiding the transmit focusing reduces the signal-to-noise ratio (SNR) and, thus, the image contrast. Slight losses in lateral resolution are also expected. However, these limitations do not affect the quality and the robust-

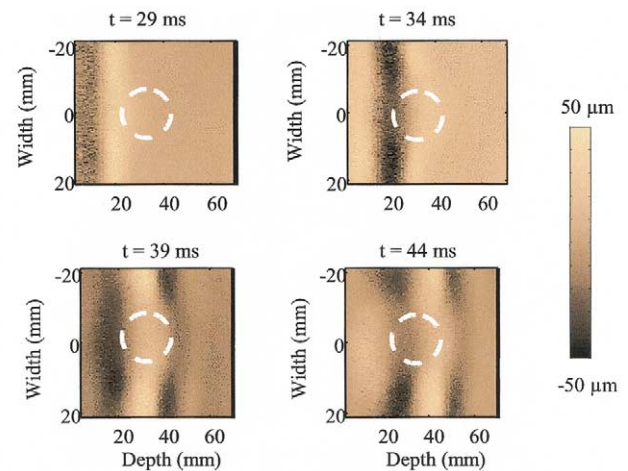


Fig. 1. Experimental displacements field in a tissue-mimicking phantom containing a 10-mm diameter inclusion. Each image corresponds to a given sampling time. The inclusion distorts the wavefront during its propagation. These spatiotemporal data are used to calculate the shear elasticity map using the inversion algorithm.

ness of the speckle motion estimation (based on a cross-correlation algorithm between successive echographic images) (Ophir et al. 1991), from which we can compute the shear propagation movie.

### Shear modulus reconstruction

In previous works (Sandrin et al. 2002a, 2002b), transient elastography was tested and validated on tissue-mimicking phantoms. Echographic images acquired during the ultrafast acquisition sequence are used to compute the movie of the shear wave propagation. Figure 1 shows an example of such a shear wave propagating through a soft medium containing a harder inclusion. The linear wavefront is clearly accelerated and distorted while passing through the inclusion. An inversion algorithm uses this spatiotemporal data to recover the Young's modulus map of the imaged medium. The inverse problem algorithm is presented in the following section and its robustness is discussed. Such a discussion is necessary to validate *in vivo* results.

Assuming the medium to be linear, isotropic, incompressible and piecewise-homogeneous, the dynamics equation can be described as follows (Olliphant et al. 2000):

$$\rho \frac{\partial^2 \vec{u}}{\partial t^2} = (\lambda + \mu) \vec{\nabla}(\vec{\nabla} \cdot \vec{u}) + \mu \vec{\nabla}^2 \vec{u}, \quad (1)$$

where  $\lambda$  and  $\mu$  are, respectively, the elastic Lamé coefficients of the bulk and shear waves,  $\vec{u}$  is the displace-

ment vector and  $\rho$  is the density. This wave equation can be split into two parts if one considers separately a null divergence (shear wave  $S$ ) or a nonrotational solution (compression waves  $P$ ). This displacement vector can be rewritten as:

$$\vec{u} = \vec{u}_p + \vec{u}_s = \vec{\nabla}\Phi + \vec{\nabla} \wedge \vec{\Psi}. \quad (2)$$

With this notation, from eqn (1) we can derive two separate equations verified by  $\phi$  and  $\vec{\psi}$ :

$$\begin{cases} \frac{\partial^2 \phi}{\partial t^2} = V_s^2 \Delta \phi \\ \frac{\partial^2 \vec{\psi}}{\partial t^2} = V_p^2 \Delta \vec{\psi} \end{cases} \quad (3)$$

with

$$V_s = \sqrt{\frac{\mu}{\rho}}$$

and

$$V_p = \sqrt{\frac{\lambda + 2\mu}{\rho}}.$$

In soft tissues, the shear modulus in an elastic medium ( $\mu \approx 10^4 Pa$ ) is much smaller than the compression modulus ( $\lambda \approx 10^9 Pa$ ) and the nonrotational displacements are propagating much faster ( $V_p = 1500 \text{ ms}^{-1}$ ) than the zero divergence ones ( $V_s = \text{a few m s}^{-1}$ ). From an experimental point of view, the  $P$  waves can be neglected in the particular case of a pulsed transient excitation because they propagate instantaneously regarding to the shear waves. Then, eqn (3) can be reduced to a single Helmholtz equation where displacement components are decoupled:

$$\rho \frac{\partial^2 u_i}{\partial t^2} = \mu \Delta u_i \quad i = x, y, z \quad (4)$$

where  $\Delta$  represents the Laplacian operator and  $u_i$  is the shear wave displacement vector. Note here that it is only true for transient excitations. In the case of monochromatic vibrations, new energy is injected by the vibrator in compressional waves at each cycle.

Because the displacement estimation is based in our application on a 1-D correlation algorithm, only displacements along the ultrasonic beam axis can be measured. Thus, we can only rely on the  $z$ -component of the

displacement vector. For this reason, the basic equation used in the inversion algorithm is reduced to:

$$\rho \frac{\partial^2 u_z}{\partial t^2} = \mu \Delta u_z \quad (5)$$

where the Laplacian term is given by:

$$\Delta u_z = \frac{\partial^2 u_z}{\partial x^2} + \frac{\partial^2 u_z}{\partial y^2} + \frac{\partial^2 u_z}{\partial z^2}. \quad (6)$$

The ultrasonic probe gives only access to a 2-D information corresponding to the echographic plane ( $x, z$ ). As a consequence, the second order derivative  $\frac{\partial^2 u_z}{\partial y^2}$  cannot be experimentally estimated and the Laplacian cannot be properly calculated. This will be a fundamental limitation of the technique until 3-D echographic systems become available. A strong assumption is then needed to perform the inversion algorithm.

$$\frac{\partial^2 u_z}{\partial y^2} \ll \frac{\partial^2 u_z}{\partial x^2} + \frac{\partial^2 u_z}{\partial z^2}. \quad (7)$$

This assumes that shear waves do not significantly diffract in the elevation direction (*i.e.*, through the image plane). To date, this assumption is common to all US-based techniques, such as static elastography (Kallel *et al.* 1997) and sonoelastography.

If this assumption is certainly wrong in sonoelasticity, where reflections on boundaries and mode conversion make the derivative  $\frac{\partial^2 u_z}{\partial y^2}$  nonnegligible, it is not necessarily the case in transient elastography. Due to its real-time capabilities, transient elastography allows the creation and imaging, without reflections from boundaries, of a shear wave that does not diffract in the  $y$ -direction. It is achieved simply by optimizing the specific shape of the mechanical vibrator. This point is addressed in the next section.

Assuming that experiments can be performed so that assumption (7) is verified, eqn (6) can be reduced into:

$$\rho \frac{\partial^2 u_z}{\partial t^2} = \mu \left( \frac{\partial^2 u_z}{\partial x^2} + \frac{\partial^2 u_z}{\partial z^2} \right). \quad (8)$$

Using this equation, it is easy to estimate locally the shear modulus in the elastic medium at each time step:

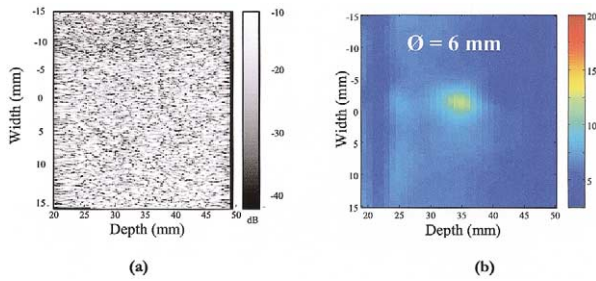


Fig. 2. Hard inclusions in a tissue-mimicking phantom (6-mm diameter). (a) Echographic image and (b) shear elasticity image. The inverse problem has been solved from the displacement field, as shown in Fig. 1, for inclusions almost 2 times harder than surrounding material. For comparison, hard tumors in the breast can be up to 8 times harder than surrounding tissue.

$$\mu(x,z) = \rho \frac{\frac{\partial^2}{\partial t^2} u_z(x,z,t)}{\frac{\partial^2}{\partial x^2} u_z(x,z,t) + \frac{\partial^2}{\partial z^2} u_z(x,z,t)}. \quad (9)$$

In the Fourier domain, the local shear modulus defined in eqn (9) can be expressed as a function of the Fourier transform (*FT*) of the Laplacian and of the second derivative of the displacement:

$$\mu(x,z) \approx \frac{\rho}{\Delta\omega} \times \int \frac{\left| FT \left\{ \frac{\partial^2}{\partial t^2} u_z(x,z,t) \right\} \right|}{\left| FT \left\{ \frac{\partial^2}{\partial x^2} u_z(x,z,t) + \frac{\partial^2}{\partial z^2} u_z(x,z,t) \right\} \right|} d\omega, \quad (10)$$

where  $\Delta\omega$  corresponds to the band width of the shear excitation. The window is chosen to obtain relevant measurement of the shear modulus; that is to say, in a frequency interval where the Laplacian is not too small. This frequency windowing acts as a regularization process before inversion.

To calculate the shear elasticity map of the phantom, eqn (10) is applied at each spatial point of the displacement movie (Fig. 1) for each frequency component of the window  $\Delta\omega$ .

One should note that, in soft tissues, the Young's modulus is directly linked to  $\mu$  by the following equation:

$$E \cong 3\mu. \quad (11)$$

The reconstructed shear elasticity image shows

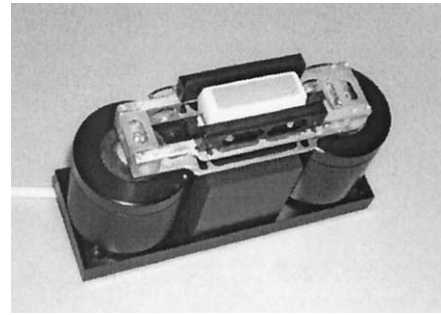


Fig. 3. Low-frequency vibrating device composed of two parallel rods, two vibrators and an ultrasonic array.

clearly the hard inclusions that cannot be observed in the conventional echographic image (Fig. 2). The inclusion shear modulus is two times higher (12.5 kPa) than the surrounding soft material (7 kPa). This experiment was conducted in an elastic and homogeneous gelatin phantom (Hall et al. 1997) containing a 6-mm twice harder inclusion.

The resolution of the technique is not limited by the wavelength of the shear wave (on the order of 1 cm), as can be the case for inverse problem in seismology. Because the displacement field and, thus, the elasticity, can be measured at each point of the ultrasonic image (that is to say, inside the medium and not at its surface as in seismology), the limitation is given by the longitudinal and lateral spatial resolution of the ultrafast scanner (about 1 mm). Figure 2 illustrates this remark for an elastic gelatin phantom: the small inclusion (6-mm diameter) is clearly defined, although its diameter is only a quarter of the shear wavelength. The complete displacement field is measured, including evanescent waves that contain details of the medium smaller than the wavelength. This is what we can call a hyperresolution system. However, if, theoretically, the ultimate resolution of the technique is given by the echographic image resolution, this is not true in clinical conditions where important noise corrupts the data. Spatial filtering is needed to get relevant data, degrading the spatial resolution. The technique can rely on a spatial resolution of 2 mm<sup>2</sup>.

### Shear wave generation

In previous works (Sandrin et al. 2002a, 2002b), the low-frequency excitation was generated using two adapted low-frequency electromagnetic vibrators (Bruel & Kjaer minishaker type 4810) connected to two parallel rods, as shown in Fig. 3. This mechanical configuration creates a linear shear wavefront in the imaging area of the transducer, as shown in Fig. 1. This configuration was chosen because of its ability to generate a shear wave that induces strong displacements in the ultrasonic

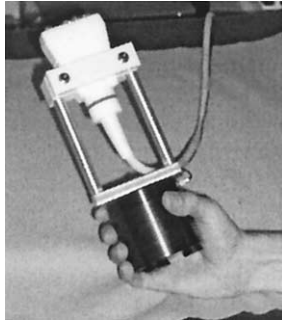


Fig. 4. Low-frequency vibrating device adapted to clinical conditions.

beam direction and that does not significantly diffract in the elevation plane. However, to adapt the experimental protocol to clinical conditions, a significant reduction of the size and weight of the vibrator device was necessary. A new device, shown in Fig. 4, was provided to the radiologist. The source of the low frequency is now the front face of the US transducer array used by the ultrafast scanner. The array is mounted on a vibrator, which makes all the system freehand. The low-frequency signal consists of a two cycles sinusoid at a 60 Hz frequency (Fig. 5). Because the array itself vibrates in this setup configuration, it is necessary to discriminate between the displacement caused by the array vibration and those caused by the shear wave propagation. This can be done by using a fixed interface echo to compensate for the array displacements (Sandrin *et al.* 2002a, 2002b). For the *in vivo* applications, the rib cage has been considered to be a fixed interface.

To analyze the consistency of the new vibrator setup, numerical simulations were performed to ensure that the inversion algorithm remains stable. Because the main limitation of the algorithm consists in its 2-D formulation, eqn (7), the shear source was chosen to minimize the diffraction effects in the elevation direction. Two shear waves are generated, respectively, by the upper and lower edges of the transducer front face. Due to symmetry considerations, these shear waves focus in the echographic plane while inducing a strong shear displacement along *z*-axis (Fig. 6). It results in a linear

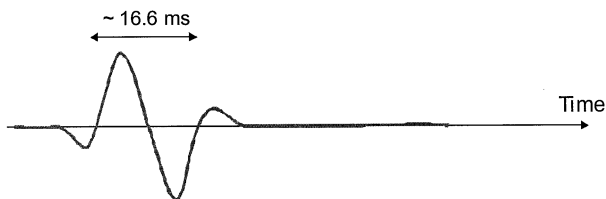


Fig. 5. Transmitted pulsed low-frequency signal (60 Hz).

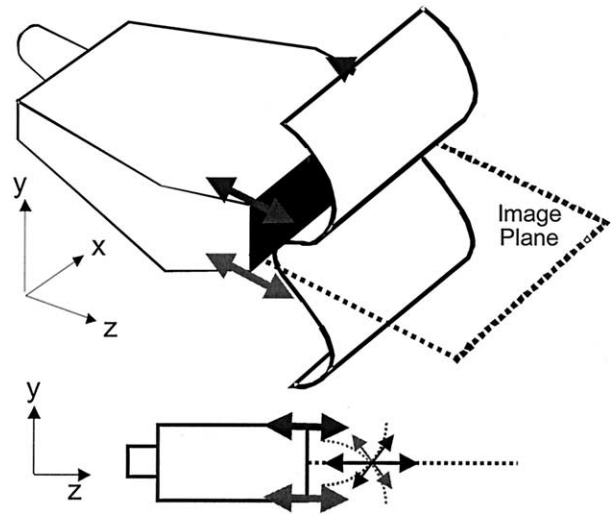


Fig. 6. Diffraction effects on the shear wavefront propagation in the near field of the probe: shear contributions due to both upper and lower edges of the probe focus in the image plane while inducing a strong longitudinal shear displacement.

shear wavefront propagating in the echographic image plane. The consequences of the diffraction effects on the elasticity estimation are quantified using a Green's function formalism simulation and compared with the usual experimental setup. A low-frequency propagating shear wave is simulated in a soft isotropic and homogeneous elastic medium. The simulation code is based on Lhémy's Green's function (Lhémy 1994) for a semi-infinite medium associated to a set of source points. The two different kind of sources tested are shown in Fig. 7.

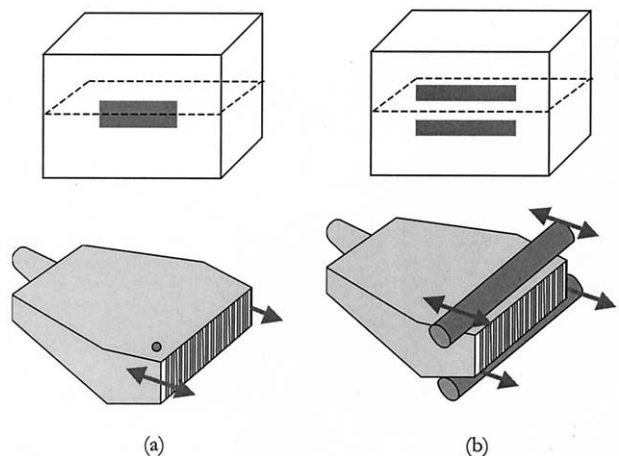
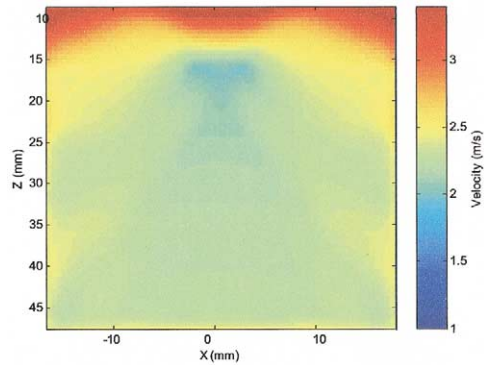
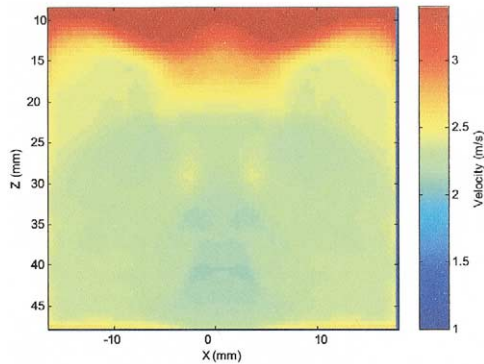


Fig. 7. The excitation sources used in the Green's function numerical simulation. (a) A rectangular  $15 \times 55 \text{ mm}^2$  source. (b) Two parallel rectangular  $10 \times 80 \text{ mm}^2$  sources. The plane presented by the dashed line is the corresponding experimental imaging zone.



(a)



(b)

Fig. 8. Velocity map for (a) A rectangular source, and (b) two parallel rectangular sources.

To mimic soft tissue properties, a medium with the following characteristics has been simulated: a compressional velocity of  $1500 \text{ ms}^{-1}$ , a shear velocity of  $2 \text{ ms}^{-1}$  and density of  $1000 \text{ kg m}^{-3}$ . The Green's function is estimated in a  $40 \times 40 \text{ mm}^2$  zone sampled with a 0.5-mm pitch. This area correspond to the  $(x, z)_{y=0}$  plane and is represented by the dashed line in Fig. 7. The displacements  $u_z$  induced in the medium were obtained by convolving the simulated Green's function by a pulse with a 60-Hz central frequency. The inverse problem is then applied to these two simulated displacements. The shear velocity maps are shown in Fig. 8. In both cases, the shear velocity is overestimated in the very near field, where eqn (6) is no more a valid assumption. Nevertheless, the shear speed estimation is valid in a large area of the image. Simulation shows that, regarding to the diffraction effects, the elasticity estimation in a homogeneous medium using the new vibrator is as good as the old one (even better in the near field). The use of the array as a vibrator appears to be an interesting solution because it gives clean reconstruction maps and is easier

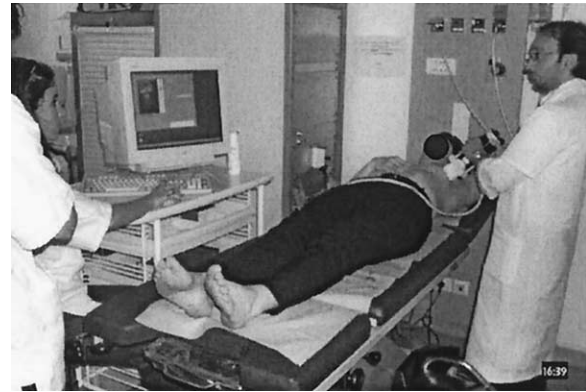


Fig. 9. *In vivo* experiments. The ultrafast scanner (middle) works as a standard echographic device and the physician (right) locates a potential region-of interest. A low-frequency impulse is then sent and 250 frames at a 3000 Hz repetition rate are recorded to memory.

to use than the old vibrator device.

Other diffraction effects in elevation, not due to the shear wave source but to inhomogeneities in the medium, could appear in the experiments (for example, at interfaces of a piecewise-homogeneous medium). This can be considered to be a fundamental limitation of the technique, as it can be for all other techniques based on 2-D US imaging. However, the technique presented gives the ability to optimize the shear wave source and, thus, to minimize the elevation diffraction by forcing the displacement field to be focused in the image plane. Both shear wave sources presented in this paragraph have this property. Other sources could be considered as will be shown in the final discussion.

## IN VIVO RESULTS

In this section, the preliminary results concerning *in vivo* validation of the transient elastography are reported. The aim of this study was to demonstrate that nodules can be detected using our ultrafast system. For this first validation, patients whose tumors were palpable (usually more than 15-mm diameter) and visible on echographic scans have been chosen. This study was realized at the Curie Institute, with the collaboration of the Radiology Department.

### Patients and study protocol

A total of 15 patients with mean age of  $61 \pm 16$  years and ages ranging between 31 and 90 years were included in this study. All subjects had a palpable breast lesion and had to undergo a biopsy and a surgical operation after the elastography evaluation. All patients gave their consent to be examined using the transient elastography technique. The histologic results showed that only

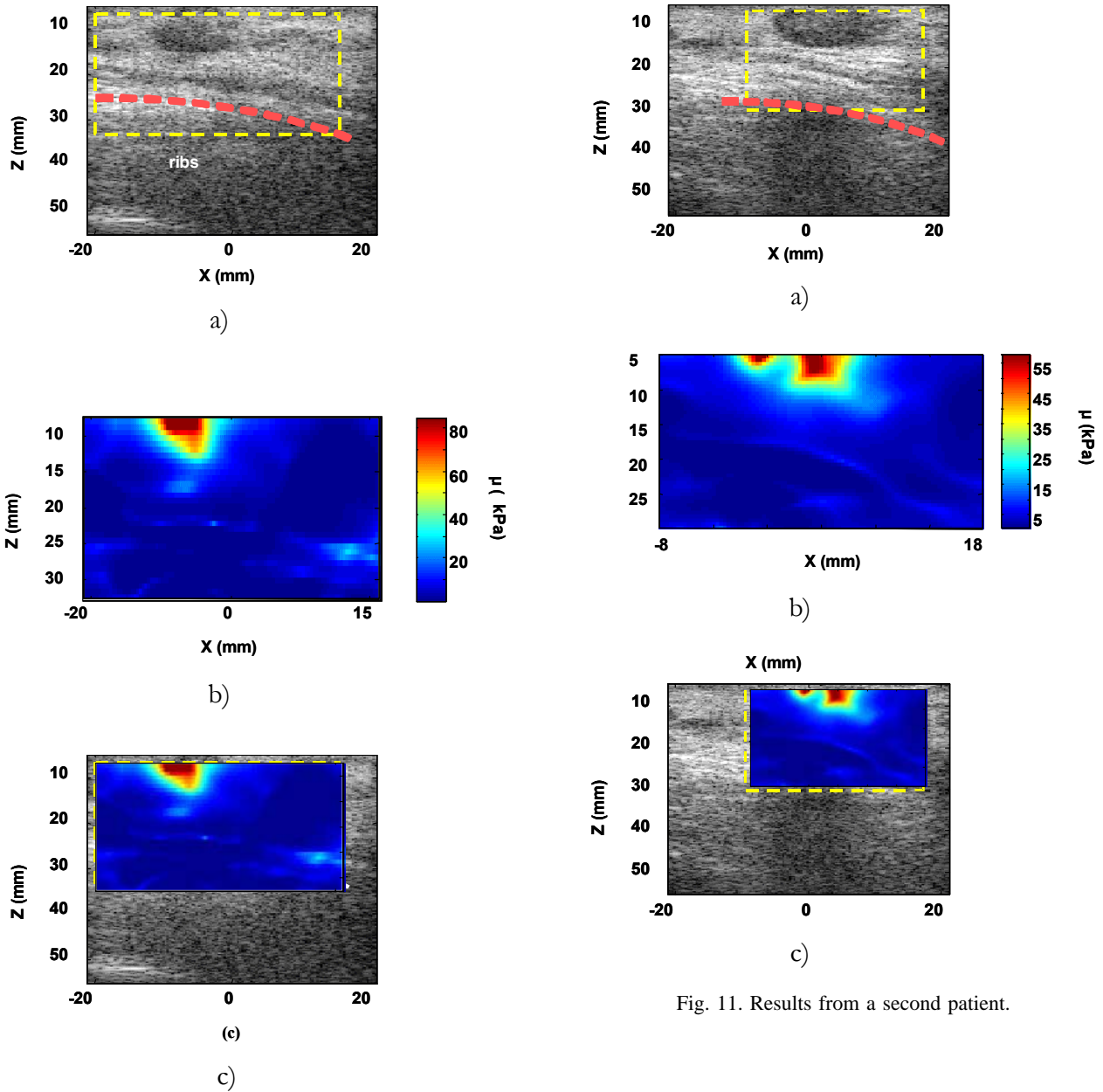


Fig. 10. (a) Comparison between echographic image and (b) a shear elasticity map of a breast. A hard tumor (adenocarcinoma) appears as a dark area on the echographic image and as red or yellow on the shear elasticity map. The elasticity maps correspond to the dashed rectangle on the echographic images. (c) The elasticity map scaled and superimposed on the echographic image.

one patient had a benign lesion and all others presented an adenocarcinoma lesion. All measurements were made by a radiologist. Each patient was lying, chest naked, on a bed (Fig. 9). First, the doctor localized the nodule by palpation, then performed an image of the tumor using

the conventional echographic mode provided by our ultrafast imaging system. Finally, when the imaging plane was considered as correct, the transient vibration was launched and, simultaneously, the ultrafast data acquisition. The echographic image and the elasticity measurements were performed using the same machine. The low-frequency impulse (a 60-Hz frequency center pulse) was exciting the breast of the patient while the ultrafast scanner recorded 250 frames at a 3000-Hz repetition rate. The total duration of a patient examination was about 10 min and three successive measurements were carried out. The ultrafast acquisition sequence was instantaneous (0.075 s), but transferring data on the computer required about 2 min.

Fig. 11. Results from a second patient.

### Elasticity measurements

For each patient, two kinds of images were performed: these were the classical echographic image and the corresponding shear modulus image. Most patients (11 among 15) presented tumors visible on the echographic images. The 4 patients corresponding to tumors that did not appear on the echographic image were eliminated from this study. Most lesions were superficial, and only 2 patients were presenting a cancerous tumor deep in the breast. The inversion algorithm described above was applied to each displacement movie of the *in vivo* measurements, resulting in an elasticity map for each patient.

Figures 10 and 11 show two examples of Young's modulus images obtained, respectively, on a 64-year-old (Fig. 10b) and a 74-year-old (Fig. 11b) volunteer and their corresponding echographic images (Fig. 10a, Fig. 11a). In both cases, nodules located on the right breast were superficial, palpable and visible in the echographic image. In Fig. 10a and 11a, the dotted curves represent the ribs. A biopsy achieved after the echographic examinations indicated that the dark area on the top was an adenocarcinoma. The inverse problem was applied in the area defined by the dashed line and resulted in the corresponding shear elasticity maps. The tumors were also visible on the elasticity images. The adenocarcinoma was found to be five and three times harder than the surrounding healthy tissue, respectively, for the first and the second patient. Its localization is not atypical and one remarks that transient elastography is able clearly to detect tumors at the surface of the breast.

Among the 11 patients examined using our transient system, 6 of them (55%) presented a hard lesion on the elasticity map. The existence and the location of these tumors were confirmed by the echographic images. These 6 patients had a superficial and palpable tumors of a few cm diameter identified during biopsy as an adenocarcinoma lesion.

## DISCUSSION

The goal of this first *in vivo* protocol was to validate, in clinical conditions, the transient elastography technique by detecting the cancerous nodule on the elasticity images. Among the 15 examined patients, 6 of them presented a clear visible tumor both on the echographic and the elasticity image. These preliminary results are very encouraging because they were the first *in vivo* elasticity images of women's breast cancer achieved by the transient elastography technique.

### Protocol limitations

The protocol was established to examine patients with a palpable tumor in an advanced stage of the dis-

ease. On 15 patients presenting palpable tumors visible on echographic images, 6 were detected by our technique. Why did we not detect tumors on the elasticity maps of all the patients chosen for this study? Two reasons explain these failures.

First, the classical echographic imaging mode achieved by our ultrasonic device, to help the radiologist while choosing a convenient imaging plane, can only rely on a very poor frame rate. Due to the limited data transfer rate, the frame rate in this classical mode was about 2 images per s. This caused a time shift between the tumor visualization on the screen and the beginning of the ultrafast acquisition mode. In 4 of the studied cases, the tumor disappeared from the imaging area, due to a movement of the physician during this time shift. These 4 patients were removed from the study, because they did not present visible tumors on the ultrafast echographic images (that were used to compute the displacement movie).

The other reason can be related to the excitation source. In fact, if the ultrasonic array surface is not completely in contact with the patient's breast, the shear wave induced by the transient push could propagate outside the imaging plane. In that particular case, the displacement movies showed a beating wave crossing the imaging plane, rather than a wave front propagation. This happened for last 5 patients whose elasticity estimation was corrupted. In other words, when there is an out-of-plane motion, the assumption

$$\frac{\partial^2 u_z}{\partial y^2} \ll \frac{\partial^2 u_z}{\partial x^2} + \frac{\partial^2 u_z}{\partial z^2}$$

is not valid and a good reconstruction of the inverse problem is not possible any more. This assumption makes the technique very sensitive to the shear wave source. A bad positioning of the transducer by the physician can easily corrupt the elasticity estimation. Moreover, even if the mechanical device were optimized for clinical conditions, it remained heavy for the physician, degrading the stability of the acquisition protocol. These limitations show the necessity of overcoming technical limitations (like the transfer rate between the ultrafast scanner and the computer) and of improving and simplifying the experimental protocol for the physician. This should increase the percentage of successful diagnostics, which reach 55% today.

### Fundamental limitations

Transient elastography has been validated as a quantitative technique for mapping shear elasticity of soft tissues. It does not provide, for now, any additional mechanical information and cannot be considered to be a

technique able to characterize tumors. In fact, elasticity is not a parameter characterizing the malignancy. To reach this level of diagnosis, the technique should be extended to other mechanical parameters like attenuation, anisotropy or nonlinearity (this has already been implemented in MRI elastography) or linked to other US capabilities such as contrast agents.

Another fundamental limitation of the technique is linked to the assumption

$$\frac{\partial^2 u_z}{\partial y^2} \ll \frac{\partial^2 u_z}{\partial x^2} + \frac{\partial^2 u_z}{\partial z^2}.$$

This limitation will be naturally overcome with 2-D arrays, but it remains today a significant challenge for the robustness of the technique. This is particularly true in strongly heterogeneous media, where the elevation component could become important. Studies on phantoms have shown that the detection of inclusions 2 to 6 times harder than surrounding tissues are not significantly affected by this effect if the shear wave generation has been properly made. Additional work on the shear wave generation could improve the stability and the robustness of the technique, in particular, in strongly heterogeneous media, and will be discussed on the next paragraph.

#### *Possible improvements and perspectives*

As mentioned above, the shear elasticity map is computed from the  $z$ -component of the displacement (normal to the array) ( $u_z$ ). Recently, we have learned how to determine the in-plane lateral component (*i.e.*, the  $x$ -component) of displacement that is perpendicular to the array axis (Tanter *et al.* 2002). This additional information should improve the final shear elasticity mapping.

Second, technical aspects should be considerably improved. The data transfer rate will be increased 100 times and the off-line computation beam-forming software should be replaced by hardware to permit real-time conventional echographic imaging.

Third, the shear wave generation will be improved to provide more robust elasticity estimation and a more versatile experimental protocol. A promising technique, that is currently under investigation at our laboratory, is the use of the acoustic radiation force to induce shear waves in the medium (Bercoff *et al.* 2002). The shear vibration is not applied externally anymore, but is remotely induced by a focused US beam. This new technique overcomes all technical limitations, such as the size or the weight of the device, because it can be realized with a single US transducer linked to the ultrafast scanner. Moreover, this technique provides a complete versatile shear wave generator because the ultrafast scanner is able to focus at any location and at any time in

the imaged medium. The shear wave shape can be adapted and optimized according to the studied medium characteristics. In particular, this could be interesting for a strongly heterogeneous medium, where several adapted shear waves could be generated at different chosen locations.

Finally, because there is no fundamental limit that prevents the use of transient elastography with 2-D ultrasonic arrays, a generalization of the current algorithm should lead to a 3-D shear elasticity mapping. As shown in MRI elastography techniques, 3-D measurements can provide quantitative estimation of tissue elasticity, nonlinearity, attenuation and anisotropy. Anticipating the commercialization of 2-D arrays, studies can already be conducted on 1.75-D US arrays that are able to provide measurements in the elevation plane. Improvements in the inversion algorithm should certainly be nonnegligible.

Compared with methods using static deformations (Ophir *et al.* 1991, 1996, 2000), the advantage of systems based on transient shear wave propagation is that no prior knowledge of the boundary conditions is needed to quantitatively estimate Young's modulus or shear elasticity. Moreover, experiments are realized in a few ms, in a time window where the compressional wave has already propagated and the shear wave has not already reached boundaries. Conversion modes and compressional terms do not need to be taken into account in the modeling equations, as in sonoelastography. This leads to a simple, robust and medium-independent inversion algorithm. Future enhancements of the technique proposed in this paper should enhance the applicability and the robustness of transient elastography and emphasize its strong potential for cancer detection.

*Acknowledgements*—The authors gratefully thank Jean-Michel Hasquenoph for his expert assistance in electronics.

## REFERENCES

- Bercoff J, Tanter M, Chaffai S, Fink M. Ultrafast imaging of beam-formed shear waves induced by the acoustic radiation force. Proceedings of the IEEE Ultrasonic Symposium, Munich, 2002.
- Catheline S, Wu F, Fink M. A solution to diffraction biases in sonoelasticity: The acoustic impulse technique. *J Acoust Soc Am* 1999; 105:2941–2950.
- Hall TJ, Bilgen M, Insana MF, Krouskop TA. Phantom materials for elastography. *IEEE Trans Ultrason Ferroelec Freq Contr* 1997; 44(6):1355–1365.
- Kallel F, Varghese T, Ophir J, Bilgen M. Nonstationary strain filter in elastography: Part II. Lateral and elevational decorrelation. *Ultrasound Med Biol* 1997;23:1357–1369.
- Levinson SF, Shinagawa M, Sato T. Sonoelastic determination of human skeletal muscle elasticity. *J Biomech* 1995;28(10):1145–1154.
- Lh emery A. An analytic expression for the transient ultrasonic field radiated by a shear wave transducer in solids. *J Acoust Soc Am* 1994;96(6):3787–3791.
- Muthupillari R, Lomas DJ, Rossman PJ, *et al.* Magnetic resonance

- elastography by direct visualisation of propagating acoustic strain wave. *Science* 1995;269:1854–1856.
- Oliphant TE, Kinnick RR, Manduca A, Ehman RL, Greenleaf JF. An error analysis of Helmholtz inversion for incompressible shear vibration elastography with application to filter-design for tissue characterization. *Proceedings of the IEEE Ultrasonic Symposium*, 2000.
- Ophir J, Cespedes I, Garra B, et al. Elastography: ultrasonic imaging of tissue strain and elastic modulus *in vivo*. *Europ J Ultrasound* 1996;3:49–70.
- Ophir J, Céspedes I, Ponnekanti H, Yasdi Y, Li X. Elastography: A quantitative method for imaging the elasticity of biological tissues. *Ultrason Imaging* 1991;13:111–134.
- Ophir J, Garra B, Kallel F, et al. Elastographic imaging. *Ultrasound in Med Biol* 2000;26(1):S23–S29.
- Parker KJ, Lerner RM. Sonoelasticity of organs: Shear waves ring a bell. *J Ultrasound Med* 1992;11:387–392.
- Sandrin L, Catheline S, Tanter M, Hennequin X, Fink M. 2D Time resolved pulsed elastography with ultrafast ultrasonic imaging. *Ultraso Imaging* 1992;21(4):259–272.
- Sandrin L, Tanter M, Catheline S, Fink M. Shear modulus imaging using 2D transient elastography. *IEEE Trans Ultrason Ferroelec Freq Control* 2002a;49(4):426–435.
- Sandrin L, Tanter M, Gennisson JL, Catheline S, Fink M. Shear elasticity probe for soft tissues with 1D transient elastography. *IEEE Trans Ultrason Ferroelec Freq Contr* 2002b;49(4):436–446.
- Shattuck D. Explososcan: A parallel processing technique for high speed ultrasound imaging with linear phased arrays. *J Acoust Soc Am* 1984;75(4):1273–1282.
- Sinkus R, Lorenzen J, Schrader D, et al. High resolution tensor MR-elastography for breast tumor detection. *Phys Med Biol* 2000;45:1649–1660.
- Tanter M, Bercoff J, Sandrin L, Fink M. Ultrafast compound imaging for 2D motion vector estimation: Application to transient elastography. *IEEE Trans Ultrason Ferroelec Freq Control* 2002;49(10):1363–1374.
- Yamakoshi Y, Sato J, Sato T. Ultrasound imaging of internal vibration of soft tissue under force vibration. *IEEE Trans Ultrason Ferroelec Freq Control* 1990;37(2):45–53.